



THERMODYNAMIC REASSESSMENT AND CALCULATION OF Fe-Ti PHASE DIAGRAM

K.C. Hari Kumar, P. Wollants, and L. Delaey
Department MTM
Katholieke Universiteit Leuven
de Croylaan 2
B-3001 Heverlee, BELGIUM

(Presented at CALPHAD XXII, Barcelona, Spain, May 1993)

ABSTRACT: A Thermodynamic description of the Fe-Ti system is obtained by a least-square optimisation of the thermochemical and phase diagram data from literature. SGTE recommended expressions for the Gibbs energies of pure elements are used. The Laves phase is modelled using a three-sublattice model that takes care of its homogeneity range. Calculated phase diagram and the thermochemical properties show good agreement with the experimental data.

INTRODUCTION

The thermodynamic properties and the phase diagram of the Fe-Ti system are of considerable technological interest. For example, information about the effect of titanium addition on the phase diagrams and thermodynamics of iron-base systems is of primary importance to the steel research. Aim of the present study is to develop reliable thermodynamic model descriptions for the stable phases of the Fe-Ti system, taking into account all available thermochemical and phase diagram data. Such descriptions are necessary for performing calculations of the phase diagrams of ternary and higher-order systems based on Fe-Ti.

The Fe-Ti system was critically assessed by [81Mur, 82Kub, 87Mur]. A number of investigators have carried out the thermodynamic assessment and calculation of Fe-Ti phase diagram. [78Kau] used subregular solution models to represent the liquid, bcc and fcc solution phases and treated FeTi and Fe₂Ti as stoichiometric compounds. The hcp phase was considered as an ideal solution. [81Mur] modelled the compound phases using Wagner-Schottky Gibbs energy functions and slightly modified the solution parameters proposed by [78Kau] for the liquid, bcc, and fcc phases. Two different descriptions were used by [81Mur] to represent the Fe-base and Ti-base bcc phases. The hcp phase was

treated as regular solution. In the work of [85Din], Fe₂Ti phase was treated as a random solution like the liquid, bcc, fcc, and hcp phases. FeTi was considered as a line compound. [87Mur] has revised the thermodynamic functions proposed by [78Kau] by incorporating new experimental data. [88Oht] have modelled the iron-rich region (up to 0.333 X_{Ti}) of the phase diagram. They also treated Fe₂Ti as stoichiometric. Gibbs energies of the pure elements used in all the above assessments are now considered to be obsolete.

THEMODYNAMIC MODELS

The equilibrium phases of the Fe-Ti system are: liquid, bcc(α), fcc(γ), hcp(ε), FeTi, and Fe₂Ti(λ, C14 Laves phase).

The liquid, bcc, fcc and hcp phases are treated as completely random solutions. The integral molar Gibbs energy(G_m^ϕ) of such a phase can be expressed as

$$G_m^\phi = \sum_{i=Fe,Ti} X_i^\phi G_i^\phi + RT \sum_{i=Fe,Ti} X_i^\phi \ln X_i^\phi + X_{Fe}^\phi X_{Ti}^\phi L_{Fe,Ti}^\phi,$$

where G_i^ϕ are the Gibbs energies of the pure elements in the structural state ϕ (ϕ =liquid, α , γ , or ϵ) and $L_{Fe,Ti}^\phi$ is the interaction term characterising the chemical contribution to the excess Gibbs energy. $L_{Fe,Ti}^\phi$ may be expanded as an n^{th} degree Redlich-Kister polynomial [48Red] as

$$L_{Fe,Ti}^\phi = \sum_{v=0}^n {}^vL_{Fe,Ti}^\phi (X_{Fe}^\phi - X_{Ti}^\phi)^v.$$

The Redlich-Kister polynomial coefficients, ${}^vL_{Fe,Ti}^\phi$, are determined by least-square optimisation of the experimental thermochemical and phase diagram data. The temperature dependence of ${}^vL_{Fe,Ti}^\phi$ may be expressed as

$${}^vL_{Fe,Ti}^\phi = a_v + b_v T + c_v T \ln T.$$

The Gibbs energy contribution due to ferromagnetic ordering of the bcc(α) phase is described using the Hillert-Jarl model [78Hil]. According to this model the Gibbs energy of magnetic ordering, ${}^{mo}G_m^\alpha$, is given by

$${}^{mo}G_m^\alpha = RT \ln(\beta^\alpha + 1) f(\tau),$$

where β^α is the average magnetic moment per atom in the bcc(α) phase, expressed in Bohr magnetons, $f(\tau)$ is a polynomial function of τ , and τ is defined as T/T_C^α ; T_C^α being the Curie temperature of the magnetic transition of the α phase. Both β^α and T_C^α may be concentration dependent.

The intermetallic compound FeTi has a narrow homogeneity range [80Dew]. In the present case it is modelled as a stoichiometric compound. This does not introduce any major errors since the homogeneity range is very narrow.

The C14 Laves Phase, $\text{Fe}_2\text{Ti}(\lambda)$, exists over a fairly wide composition range. For example, at 1473 K it exists between 26.4 and 34.9 at.% of Ti [59Mur]. Modelling such a phase as a stoichiometric compound [78Kau] or as a completely disordered solution phase [85Din] is unrealistic. The problem can be resolved if one uses a suitable sublattice model [70Hil, 81Sun] to represent the phase. In the present study a three-sublattice model based on the ideal stoichiometric compound $(\text{Fe})_2(\text{Ti})_4(\text{Fe})_6$ is selected. This rationalises 12 atoms per unit cell and three sublattices having co-ordination numbers (CN) 12, 16, and 12 respectively. It is suggested that by approximating Gibbs energies of a sublattice with CN 12 to that of elements in their fcc structure and one with CN 14 or higher to that of elements in their bcc structure, the resulting thermodynamic description may become simple [86And]. In order to account for the homogeneity range, one must introduce defects to these sublattices. Defects could be either a second atom occupying the positions of the other (i.e. Fe substituting the positions of Ti or vice versa) or vacancies substituting for Fe and Ti atoms. Since Ti atoms are considerably larger than Fe atoms ($R_{\text{Ti}} = 2.00\text{\AA}$, $R_{\text{Fe}} = 1.72\text{\AA}$), the possibility of Ti substituting for Fe is ruled out. However, Fe being smaller than Ti, it is realistic to assume that some positions of Ti are occupied by Fe. This accommodates all compositions falling below the ideal composition $0.333 X_{\text{Ti}}$. In order to take care of compositions above the ideal composition, it is necessary and sufficient to introduce vacancies (va) into one of the sublattices containing Fe. Thus the sublattice model $(\text{Fe},\text{va})_2:(\text{Ti},\text{Fe})_4:(\text{Fe})_6$ is chosen to represent the Laves phase. This model can account for compositions up to $0.4 X_{\text{Ti}}$ (corresponding to the hypothetical compound $(\text{va})_2(\text{Ti})_4(\text{Fe})_6$). Gibbs energy per mole of formula unit of λ , ($^{\circ}\text{G}^{\lambda}$), is given by

$$\begin{aligned} ^{\circ}\text{G}^{\lambda} = & {}^1y_{\text{Fe}}^{\lambda}({}^2y_{\text{Ti}}^{\lambda} {}^{\circ}\text{G}_{\text{Fe:Ti:Fe}}^{\lambda} + {}^2y_{\text{Fe}}^{\lambda} {}^{\circ}\text{G}_{\text{Fe:Fe:Fe}}^{\lambda}) + {}^1y_{\text{va}}^{\lambda}({}^2y_{\text{Ti}}^{\lambda} {}^{\circ}\text{G}_{\text{va:Ti:Fe}}^{\lambda} + {}^2y_{\text{Fe}}^{\lambda} {}^{\circ}\text{G}_{\text{va:Fe:Fe}}^{\lambda}) + \\ & RT[2({}^1y_{\text{Fe}}^{\lambda} \ln {}^1y_{\text{Fe}}^{\lambda} + {}^1y_{\text{va}}^{\lambda} \ln {}^1y_{\text{va}}^{\lambda}) + 4({}^2y_{\text{Ti}}^{\lambda} \ln {}^2y_{\text{Ti}}^{\lambda} + {}^2y_{\text{Fe}}^{\lambda} \ln {}^2y_{\text{Fe}}^{\lambda})] + \\ & {}^1y_{\text{Fe}}^{\lambda} {}^1y_{\text{va}}^{\lambda}({}^2y_{\text{Ti}}^{\lambda} L_{\text{Fe,va:Ti:Fe}}^{\lambda} + {}^2y_{\text{Fe}}^{\lambda} L_{\text{Fe,va:Fe:Fe}}^{\lambda}) + \\ & {}^2y_{\text{Ti}}^{\lambda} {}^2y_{\text{Fe}}^{\lambda}({}^1y_{\text{Fe}}^{\lambda} L_{\text{Fe:Ti,Fe:Fe}}^{\lambda} + {}^1y_{\text{va}}^{\lambda} L_{\text{va:Ti,Fe:Fe}}^{\lambda}) + \\ & {}^1y_{\text{Fe}}^{\lambda} {}^1y_{\text{va}}^{\lambda} {}^2y_{\text{Ti}}^{\lambda} {}^2y_{\text{Fe}}^{\lambda} L_{\text{Fe,va:Ti,Fe:Fe}}^{\lambda} \end{aligned}$$

where $^s y_i^{\lambda}$ is the site fraction of component i in sublattice s , $^{\circ}\text{G}_{\text{I}(0)}^{\lambda}$ is the Gibbs energy of the zeroth order component array $\text{I}(0)$, and $L_{\text{I}(Z)}^{\lambda}$ is the interaction term for the component array $\text{I}(Z)$ of Z^{th} order ($Z=1$ or 2). The composition dependence of the first four L terms may be expressed as an n^{th} degree Redlich-Kister polynomial in appropriate $^s y_i^{\lambda}$. For example,

$$L_{\text{Fe,va:Ti:Fe}}^{\lambda} = \sum_{v=0}^n v L_{\text{Fe,va:Ti:Fe}}^{\lambda} ({}^1y_{\text{Fe}}^{\lambda} - {}^1y_{\text{va}}^{\lambda})^v.$$

The term $L_{\text{Fe,v.a.:Ti,Fe:Fe}}^{\lambda}$ is assumed to be independent of composition. In the present case all $L_{i(\text{Zr})}^{\lambda}$ terms are assumed to be zero due to lack of sufficient experimental thermochemical information.

After the completion of this study we came across a recent work by [93Zen], where a similar approach was used to model the C14, C15, and C36 Laves phases (Cr_2Zr) of Cr-Zr system. They modelled the C15 modification using the two-sublattice model $(\text{Cr,Zr})_2(\text{Zr,Cr})_1$, whereas C14 and C36 modifications were modelled using the three-sublattice model $(\text{Cr})_2(\text{Zr,Cr})_4(\text{Cr,Zr})_6$. These formalisms involve substitution of smaller Cr atoms by bigger Zr atoms.

GIBBS ENERGIES OF PURE ELEMENTS

The most recent SGTE recommendations of Gibbs energy expressions for the pure elements in each phase ($^{\circ}\text{G}_i^{\circ}$) are used [91Din]. These are not reproduced here to save space.

OPTIMISATION OF THE MODEL PARAMETERS

A selected set of thermodynamic and phase diagram data was used for the least-square optimisation of Gibbs energy model parameters. These are summarised in Table 1 and 2 respectively. Critical assessments by [81Mur, 82Kub, 87Mur] were used as a guide for selecting the experimental phase diagram data.

An expression for the concentration dependence of T_c^{α} was obtained from an analysis of the experimental data of [59Arr, 73Pal]. β^{α} was assumed to decrease linearly from the value of 2.22 for pure α -Fe.

The optimisation was started by a weighted least-square fitting of an optimum-degree Redlich-Kister polynomial to the heat of mixing data for the liquid reported by [81Est, 84Bat, 91Wan]. The procedure SN007F of the SOLUT software library [93Har1] which automatically determines the most appropriate degree of the polynomial, was used for the purpose. It was found that the expression $X_{\text{Ti}}X_{\text{Fe}}(-69620)$ J/mol gave the best fit to the data (correlation coefficient, $R = 0.972$). This is very close to the expression predicted by Miedema's model [83Nie], which is $X_{\text{Ti}}X_{\text{Fe}}(-67304)$ J/mol. In order to find the model parameters describing the excess entropy of the liquid, it was decided to apply Tanaka's model [93Tan] to the experimental heat of mixing data. This was accomplished by using a recently developed computer program of [93Har2]. The generated excess entropy values were fitted to an optimum-degree Redlich-Kister polynomial. This led to a value of $-69620 + 9.225T$ J/mol for ${}^0L_{\text{Fe,Ti}}^{\text{Liquid}}$. Activity values predicted using this suggests that the experimental activity data of [75Fur] are more reliable than those of [74Wag] (see discussion). This observation was taken into account during the final optimisation.

TABLE 1: Summary of Experimental Thermodynamic Data Used in the Optimisation of Model Parameters		
Reference	Experimental technique used	Quantity measured
[55Kub]	Calorimetry	Heat of formation of FeTi
[70Fru]	EMF studies	a_{Ti} in liquid alloys
[74Wag]	Mass spectrometry	Partial excess Gibbs energies of Fe and Ti in liquid alloys
[75Fur]	Mass spectrometry	a_{Ti} in liquid alloys
[81Esl]	Calorimetry	Heat of mixing of liquid alloys
[83Gac]	Calorimetry	Heat of formation of FeTi and λ
[84Bat]	Calorimetry	Heat of mixing of liquid alloys
[85Din]	Calorimetry	Heat of formation of FeTi and λ
[91Wan]	Calorimetry	Heat of mixing of liquid alloys

TABLE 2: Summary of Experimental Phase Diagram Data Used in the Optimisation of Model Parameters		
Reference	Experimental technique used	Phase boundary investigated
[51Mcq]	Metallography	Ti-rich transus
[51Wor]	Metallography	Ti-rich transus [#] , (FeTi+ α)/ α
[52Roe]	Dilatometry	γ -loop
[52Thy]	Thermal analysis, Metallography	Ti-rich liquidus [#] , Ti-rich transus, (FeTi+ α)/ α
[57Hel]	Thermal analysis	Liquidus, Fe-rich solidus, γ -loop
[59Mol]	Diffusion studies	γ -loop
[59Mur]	Metallography, X-ray	(α + λ)/ λ , λ /(λ +FeTi)
[62Spe]	Volume fraction	Fe-rich solvus
[63Wad]	Dilatometry	γ -loop
[66Abr]	X-ray	Fe-rich solvus
[66Fis]	Magnetic susceptibility, Volume fraction of austenite	γ -loop
[67Rau]	Metallography	Ti-rich solvus
[76Bla]	Mössbauer spectra	Ti-rich solvus
[79Mat]	Electrical resistivity	Ti-rich solvus
[80Dew]	EPMA, X-ray	λ /(λ +FeTi), (λ +FeTi)/FeTi, FeTi/(FeTi+ α), (FeTi+ α)/ α
[81Tak]	EPMA, X-ray	Fe-rich solvus

[#] Not used in the optimisation

An approximate value of ${}^0L_{Fe,Ti}^{\alpha}$ was obtained by analysing the α /liquid allotropic phase boundary (T_0 -line) using the data reported by [57Hel] and the assessed values of the co-ordinates of the two eutectic reactions. Similarly, an analysis of the allotropic phase boundary α/γ , using the experimental tie-line data concerning the γ -loop by [66Fis], helped in finding an approximate value for ${}^0L_{Fe,Ti}^{\gamma}$. Approximate values for the enthalpy parts of the Gibbs energy expressions for FeTi and λ were obtained from the heat of formation data reported by [55Kub, 83Gac, 85Din].

Initial estimates of the model parameters obtained as explained above and zero values for the rest served as good guess values in the least-square optimisation using the computer program BINGSS developed by [77Luk]. Altogether 181 pieces of data were used in the optimisation. Since the Fe-rich region of the phase diagram is better established than the Ti-rich region, the phase diagram data in the Fe-rich region were given more weight during the optimisation. The final estimate of the model parameters for all stable phases of the Fe-Ti system are listed in Table 3. Parameters not listed in the table are assumed to have zero values.

DISCUSSION

In Fig. 1 the calculated enthalpy of mixing of the liquid phase is compared with the corresponding experimental values. The calculated curve is closer to that of [81Esl, 84Bat] in the Fe-rich corner of the diagram, whereas around 0.3 X_{Ti} it is more close to the data of [91Wan]. The activities calculated at 1873 K (1600 °C) are compared with those reported in the literature and those predicted using Tanaka's model [93Tan] (see Fig. 2). The activity data reported by [70Fru] using EMF method were recalculated using a more appropriate EMF value (−600.6 mV) for the cell Ti(solid)-TiO(solid), which is also shown in Fig. 2. Our analysis reveals that the activity data of [75Fur] is more reliable than those of [74Wag]. In Table 4 the calculated heat of formation for FeTi and λ is compared with various experimental values from the literature. Agreement of values is better for FeTi than for λ phase. Calculations show that the heat of formation of λ is more negative than that of FeTi. This contradicts with the findings of [85Din]. However, this trend is in perfect agreement with the phase diagram features.

The calculated phase diagram is compared with various experimental phase boundary data, in Fig. 3. Calculated co-ordinates of the special points are also indicated. Congruent melting of λ occurs at 1700 K (1427 °C) corresponding to 0.336 X_{Ti} . The peritectic formation of FeTi ($\lambda + \text{Liquid} \rightleftharpoons \text{FeTi}$) takes place at 1589 K (1316 °C). Except for the eutectoid reaction ($\alpha \rightleftharpoons \text{FeTi} + \epsilon$) the co-ordinates of all other invariant reactions are reproduced within the limits of experimental accuracy. The calculated temperature of the eutectoid reaction is about 27 K lower than that proposed by [67Rau, 87Mur]. This is to some extent due to the impossibility of fitting the experimental Ti-rich transus data reported by [51Mcq, 51Wor, 52Thy]. A calculation of the initial slope of the transus, $(dT/dX_{Ti})_{\text{transus}}$ using the van't Hoff relationship, assuming a vertical solvus, suggests a value of 2660 K/100 at.% Ti. The data of [51Mcq], however, indicate a value of 1714 K/100 at.% Ti.

TABLE 3: Optimised Values of Model Parameters*	
Liquid, (in J/mol of atoms)	
${}^0L_{Fe,Ti}^{Liquid} = -67589 + 9.809T$	
${}^1L_{Fe,Ti}^{Liquid} = -4731$	
BCC (α)	
${}^0L_{Fe,Ti}^{\alpha} = -57943 + 14.954T$, (in J/mol of atoms)	
${}^1L_{Fe,Ti}^{\alpha} = -6059$, (in J/mol of atoms)	
$T_C^{\alpha} = +1043X_{Fe} + 637.790X_{Fe}X_{Ti}$, (in K)	
$\beta^{\alpha} = +2.22X_{Fe}$, (in Bohr magneton)	
FCC (γ), (in J/mol of atoms)	
${}^0L_{Fe,Ti}^{\gamma} = -50304 + 5.487T$	
HCP (ϵ), (in J/mol of atoms)	
${}^0L_{Fe,Ti}^{\epsilon} = +15132 - 8.668T$	
FeTi, (in J/mol of FeTi)	
${}^0G_{Fe,Ti}^{FeTi} - {}^0G_{Fe}^{HBCC} - {}^0G_{Ti}^{HCP} = -53650 + 7.495T + H_{Fe}^{SER} + H_{Ti}^{SER}$	
Laves Phase (λ), (in J/mol of λ)	
${}^0G_{Fe,Ti:Fe}^{\lambda} - 8 {}^0G_{Fe}^{FCC} - 4 {}^0G_{Ti}^{BCC} = -429782 + 120.875T + 8H_{Fe}^{SER} + 4H_{Ti}^{SER}$	
${}^0G_{Fe:Fe:Fe}^{\lambda} - 8 {}^0G_{Fe}^{FCC} - 4 {}^0G_{Fe}^{HBCC} = +69869 + 12H_{Fe}^{SER}$	
${}^0G_{va:Ti:Fe}^{\lambda} - 6 {}^0G_{Fe}^{FCC} - 4 {}^0G_{Ti}^{BCC} = -356573 + 109.065T + 6H_{Fe}^{SER} + 4H_{Ti}^{SER}$	
${}^0G_{va:Fe:Fe}^{\lambda} - 6 {}^0G_{Fe}^{FCC} - 4 {}^0G_{Fe}^{HBCC} = +60724 + 10H_{Fe}^{SER}$	

* Optimisation was performed using the computer program BINGSS [77Luk]
SER denotes Stable Element Reference

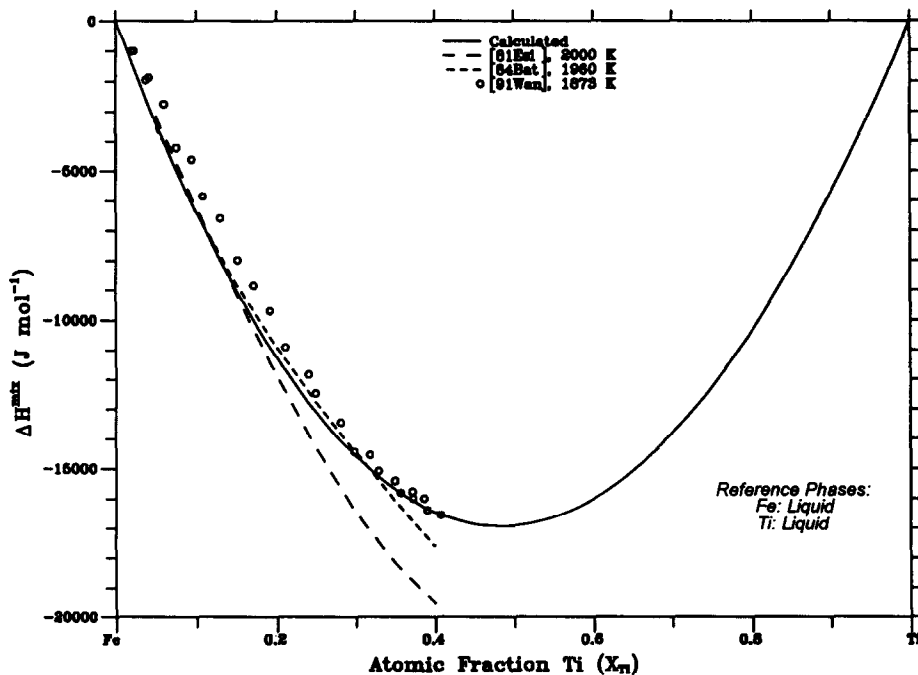


FIG. 1 Enthalpy of Mixing of Liquid Fe-Ti Alloys

TABLE 4: Comparison of Calculated Heats of Formation with Experimental Data

Phase	Reference Phases		T (K)	X_{Ti}	Calculated (J/mol)	Experimental (J/mol)	Source
	Fe	Ti					
FeTi	bcc	hcp	298	0.5	-22250	-20292	[55Kub]
	fcc	bcc	1440	0.5	-27544	-31000	[83Gac]
	bcc	hcp	973	0.5	-24192	-29588	[85Din]
	fcc	bcc	1513	0.5	-27297	-27807	[85Din]
λ	fcc	bcc	1514	0.333	-34331	-27600	[83Gac]
	bcc	hcp	973	0.333	-30890	-21294	[85Din]
	fcc	bcc	1413	0.333	-34557	-25394	[85Din]

TABLE 5: Comparison of Calculated Invariant Equilibrium with Literature Values

Reaction	Reaction Type	Compositions of the Respective Phases, X_{Ti}	T(K)	Reference
Liquid $\rightleftharpoons \lambda$	Congruent Melting	0.336	1700	Calculated
			1803	[54Nis] [#]
			1753	[56Kor] [#]
		0.329	1700	[57Hel]
			1700	[82Kub]*
		0.333	1700	[87Mur]*
λ +Liquid \rightleftharpoons FeTi	Peritectic	0.357, 0.511, 0.500	1589	Calculated
			1590	[54Nis]
			1571	[56Kor] [#]
			1583	[59Mur]
			1589	[57Hel]
			1588	[65Bor] [#]
			1590	[82Kub]*
		0.352, 0.505, 0.497	1590	[87Mur]*
Liquid $\rightleftharpoons \alpha$ + λ	Eutectic	0.155, 0.100, 0.265	1566	Calculated
			1613	[54Nis] [#]
			1571	[56Kor] [#]
		0.160, 0.098, 0.333	1562	[57Hel]
			1598	[65Bor] [#]
		0.160, 0.098,	1563	[82Kub]*
		0.160, 0.100, 0.276	1562	[87Mur]*
Liquid \rightleftharpoons FeTi+ α	Eutectic	0.711, 0.500, 0.770	1351	Calculated
		0.712,,	1353	[52Thy]
			1353	[54Nis] [#]
			1363	[65Bor] [#]
		\approx 0.710, 0.518,	1358	[82Kub]*
		0.705, 0.525, 0.790	1358	[87Mur]*
α \rightleftharpoons FeTi+ ϵ	Eutectoid	0.878, 0.500, 0.99967	841	Calculated
			\approx 868	[67Rau]
			\approx 873	[79Mat]
		0.870,,	863	[82Kub]*
		0.850, 0.510, 0.9996	868	[87Mur]*

* Assessed values

[#] Not used in the optimisation

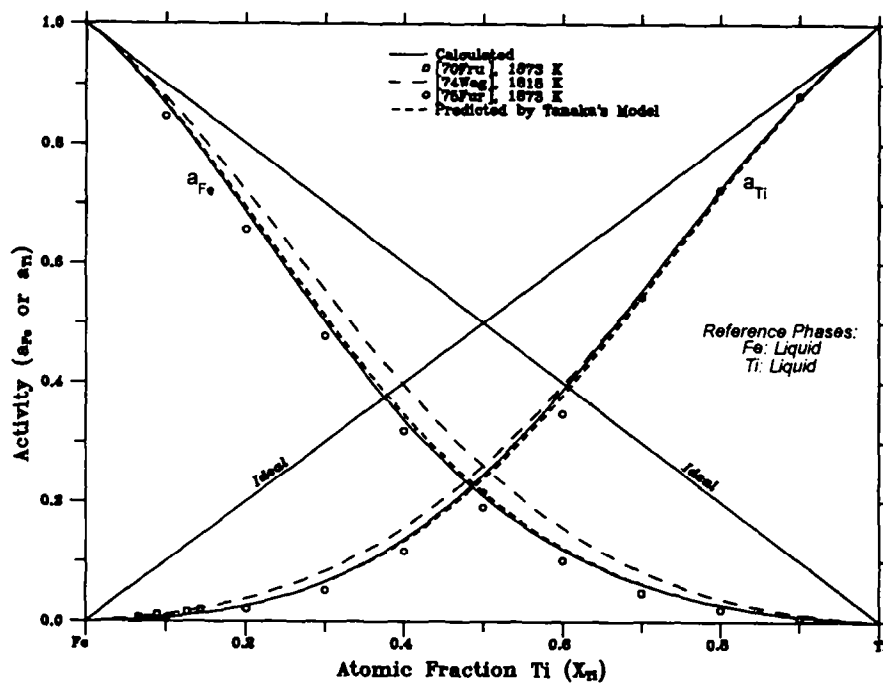


FIG. 2 Activities of Fe and Ti in Liquid Fe-Ti Alloys at 1873 K

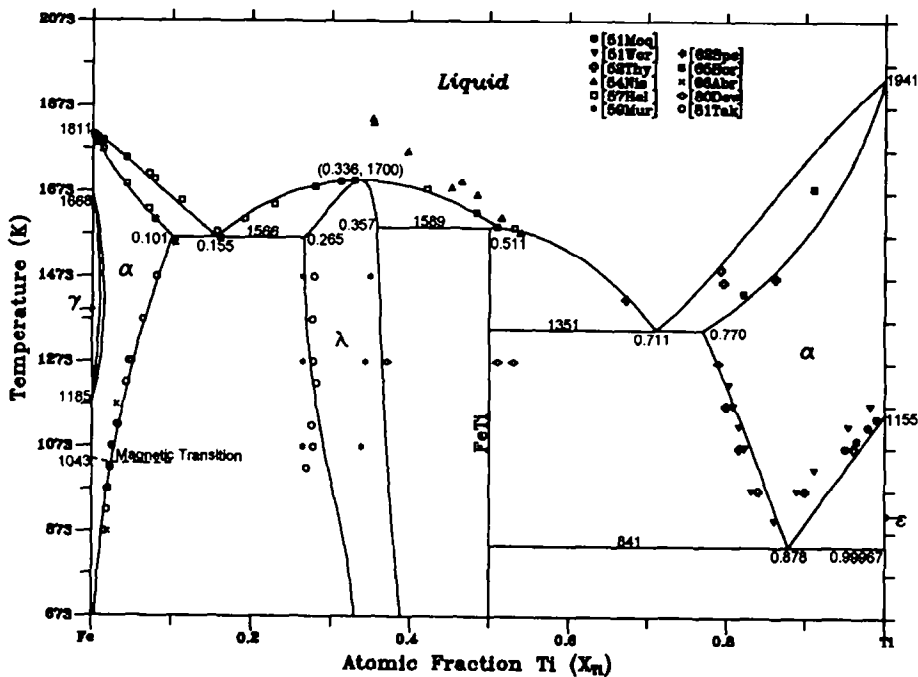


FIG. 3 Computed Fe-Ti Phase Diagram

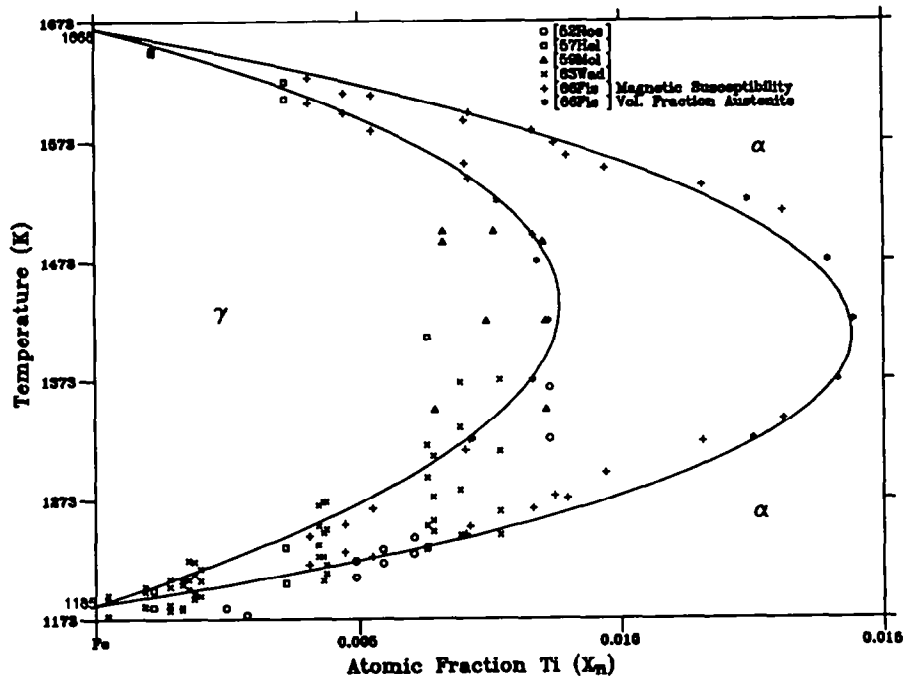


FIG. 4 γ -loop of Fe-Ti System

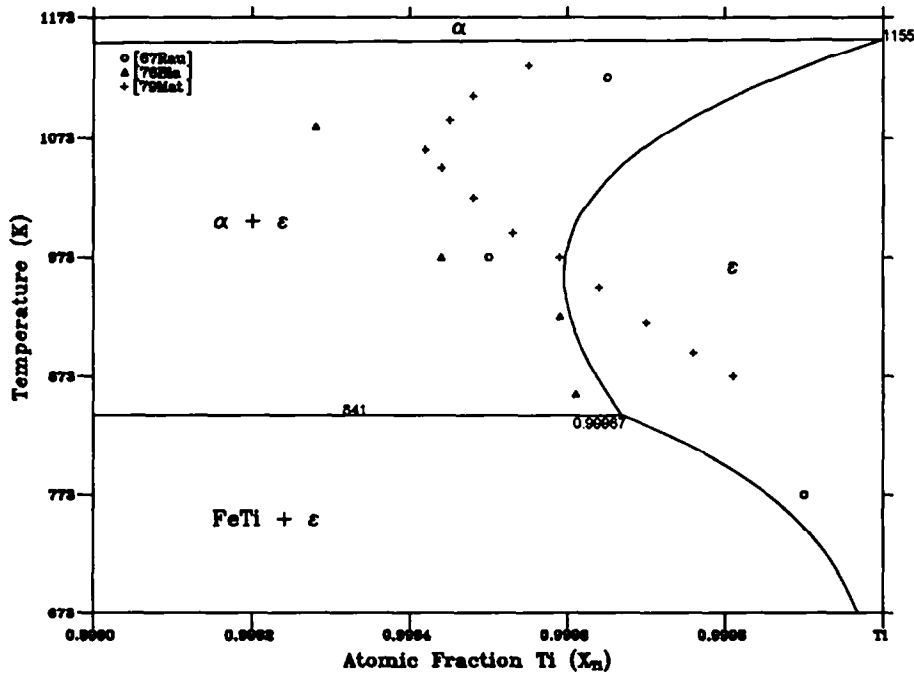


FIG. 5 Retrograde Solubility Behaviour of Fe In hcp-Ti(ϵ)

This explains the difficulty in fitting these data. Table 5 compares the co-ordinates of calculated invariant points with various literature values.

The fit is better in the Fe-rich region of the phase diagram than in the Ti-rich region. The computed phase diagram shows that the ferromagnetic transition of the Fe-rich α phase at about 1043 K (770 °C) significantly influences the disposition of $(\alpha+\lambda)/\lambda$ phase boundary in this temperature region. Fig. 4 shows the calculated γ -loop along with the experimental results from literature. The maximum solubility of Ti in γ -Fe is about 0.009 X_{Ti} corresponding to about 1423 K (1150 °C). In Fig. 5 the Ti-rich region of the phase diagram is shown, depicting the retrograde solubility behaviour of Fe in the hcp(ϵ) phase. During the optimisation it was observed that, without introducing an unreasonable value for $^0L_{Fe,Ti}^{\epsilon}$ it was impossible to fit the experimental data of [67Rau, 76Bla, 79Mat]. The computed solubility maximum is about 100 K lower than the corresponding experimental value of [79Mat]. However, the assessed diagram of [87Mur] agrees well with the phase boundaries shown in Fig. 5.

ACKNOWLEDGEMENTS

The authors wish to thank Dr. H.L. Lukas of the Max-Planck-Institute, Stuttgart, Germany, for providing the software used in the present work. The financial support offered to the Department MTM of the Katholieke Universiteit Leuven by the Flemish Ministry of Education and by the Research Council of Katholieke Universiteit Leuven, in the framework of "GOA-Action", is gratefully acknowledged. One of the authors (KCH) also thanks Prof. V. Raghavan of the Centre for Materials Science and Technology, Indian Institute of Technology Delhi, India, for providing some key references used in this work.

REFERENCES

- [48Red]: O. Redlich and A.T. Kister, *Ind. Eng. Chem.*, **40**, 345(1948).
- [51Mcq]: A.D. McQuillan, *J. Inst. Met.*, **79**, 73(1951).
- [51Wor]: H.W. Worner, *J. Inst. Met.*, **79**, 173(1951).
- [52Roe]: W.P. Roe and W.P. Fisher, *Trans. ASM*, **44**, 1030(1952).
- [52Thy]: R.J. van Thyne, H.D. Kessler, and M. Hansen, *Trans. ASM*, **44**, 974(1952).
- [54Nis]: H. Nishimura and K. Kamel, *Bull. Eng. Res. Inst., Kyoto Univ.*, **6**, 38(1954).
- [55Kub]: O. Kubaschewski and W.A. Dench, *Acta Metall.*, **3**, 339(1955).
- [56Kor]: I.I. Kornilov and N.G. Boriskina, *Dokl. Akad. Nauk SSSR*, **108**, 1083(1956).
- [57Hel]: A. Hellawell and W. Hume-Rothery, **249**, 51(1957).
- [59Arr]: A. Arrot and J.E. Noakes, *J. Applied Physics (Supplement)*, **30**, 97S(1959).
- [59Mol]: S.H. Moll and R.E. Ogilvie, *Trans. AIME*, **215**, 613(1959).
- [59Mur]: Y. Murakami, H. Kimura, and Y. Nishimura, *Trans. Nat. Res. Inst. Met. (Tokyo)*, **1**, 7(1959).
- [62Spe]: G.R. Speich, *Trans. AIME*, **224**, 850(1962).
- [63Wad]: T. Wada, *J. Japan Inst. Metals*, **27**, 119(1963).
- [65Bor]: N.G. Boriskina and I.I. Kornilov, *Sb. Nouyve Titanov. Splanov. Moscow, Izd. Nauk*, **6**, 61(1965).

- [66Abr]: E.P. Abrahamson and S.L. Lopata, *Trans. AIME*, **236**, 76(1966).
- [66Fis]: W.A. Fischer, K. Lorenz, H. Fabritius, A. Hoffmann, and G. Kalwa, *Arch. Eisenhütten.*, **37**, 79(1966).
- [67Rau]: E. Raub, Ch. J. Raub, E. Röschel, V.B. Compton, T.H. Geballe, and B.T. Matthias, *J. Less-Common Metals*, **12**, 36(1967).
- [70Hil]: M. Hillert and L.I. Staffansson, *Acta Chem. Scand.*, **24**, 3618(1970).
- [70Fru]: R.J. Fruehan, *Metall. Trans.*, **1**, 3403(1970).
- [73Pal]: R.J. Palma and K. Schröder, *J. Less-Common Metals*, **31**, 249(1973).
- [74Wag]: S. Wagner and G.R. St. Pierre, *Metall. Trans.*, **5**, 887(1974).
- [75Fur]: T. Furukawa and E. Kato, *Tetsu-to-Hagané*, **61**, 3060(1975).
- [76Bla]: A. Blaesius and U. Gonser, *J. Phys. Colloq.*, **37**, C6-397(1976).
- [77Luk]: H.L. Lukas, E.-Th. Henig, and B. Zimmermann, *Calphad*, **1**, 225(1977).
- [78Hil]: M. Hillert and M. Jarl, *Calphad*, **2**, 227(1978).
- [78Kau]: L. Kaufman and H. Nesor, *Calphad*, **2**, 55(1978).
- [79Mat]: J. Matyka, F. Faudot, and J. Bigot, *Scr. Metall.*, **13**, 645(1979).
- [80Dew]: D. Dew-Hughes, *Metall. Trans. A*, **11**, 1219(1980).
- [81Esi]: Yu. O. Esin, M.G. Valishev, and A.F. Ermakova, *Izv. Akad. Nauk SSSR, Metall.*, (3), 30(1981).
- [81Mur]: J.L. Murray, *Bull. Alloy Phase Diagrams*, **2**, 320(1981).
- [81Sun]: B. Sundman and J. Ågren, *J. Phys. Chem. Solids*, **42**, 297(1981).
- [81Tak]: T. Takayama, M.Y. Wey, and T. Nishizawa, *Trans. Jpn. Ins. Met.*, **22**, 315(1981).
- [82Kub]: O. Kubaschewski, *"Iron-Binary Phase Diagrams"*, Springer-Verlag (Berlin), 152(1982).
- [83Gac]: J.C. Gachon and J. Hertz, *Calphad*, **7**, 1(1983).
- [83Nie]: A.K. Niessen, F.R. de Boer, R. Boom, P.F. de Châtel, W.C.M. Mattens, and A.R. Miedema, *Calphad*, **7**, 51(1983).
- [84Bat]: G.I. Batalin, V.P. Kurach, and V.S. Sudavtsova, *Zhurnal Fizicheskoi Khimii*, **58**, 481(1984).
- [85Din]: A.T. Dinsdale, T.G. Chart, and F.H. Putland, *NPL Report DMA (A) 96*, (1985).
- [86And]: J.O. Andersson, A.F. Guillermet, M. Hillert, and B. Sundman, *Acta Metall.*, **34**, 437(1986).
- [87Mur]: J.L. Murray, *"Phase Diagrams of Binary Titanium Alloys"*, J.L. Murray Ed., ASM International, Metals Park, OH, 99(1987).
- [88Oht]: H. Ohtani, T. Tanaka, M. Hasabe, and T. Nishizawa, *Calphad*, **12**, 225(1988).
- [91Din]: A.T. Dinsdale, *Calphad*, **15**, 317(1991).
- [91Wan]: H. Wang, R. Lück, and B. Predel, *Z. Metallkd.*, **82**, 659(1991).
- [93Har1]: K.C. Hari Kumar, B. Halleman, P. Wollants, and L. Delaey, *Programs and Abstracts, CALPHAD XXII, Catalonia, Spain, May 16-21 (1993)*.
- [93Har2]: K.C. Hari Kumar, P. Wollants, and L. Delaey, *Programs and Abstracts, CALPHAD XXII, Catalonia, Spain, May 16-21 (1993)*.
- [93Tan]: T. Tanaka, N.A. Gokcen, Z.I. Morita, and T. Iida, *Z. Metallkd.*, **84**, 192(1993).
- [93Zen]: Zeng Kejun, M. Härmäläinen, and K. Lilius, *Calphad*, **17**, 101(1993).